On the Periodic Redshifts of Galaxies and Associated QSOs

R. Wayte

29 Audley Way, Ascot, Berkshire, SL5 8EE, England, UK

e-mail: rwayte@googlemail.com

Abstract: The observed periodicity of intrinsic-redshift in galaxies and associated QSOs has been explained by using the previous theory of a gravito-cordic field for galaxies. The quantisation period is a function of the atomic fine structure constant and it depends upon an action principle operating around galactic orbits and QSOs, or between field galaxies. The calculated separations of many QSO-galaxy pairs have been found to fit a diffusion law distribution, which suggests that associated QSOs were ejected from parent galaxies.

Key words: galaxies:active---quasars:general--- redshifts

PACS Codes: 98.54.-h, 98.54.Aj, 98.62.Py

1.   Introduction

In this paper, the theory of an auxiliary gravito-cordic field previously developed for galaxies (Wayte, 2010a, Paper 1), will be extended to explain quantisation of intrinsic-redshifts in associated QSOs, groups of galaxies, and field galaxies. A large body of evidence for intrinsic-redshift has been accumulated over 40 years, but no theory has yet been accepted; see the review by Ratcliffe (2009). The theory proposed by Narlikar and Arp (1993) depends on matter creation within galaxies, followed by ejection, but it is not compatible with the current Big Bang model of the universe. Here, a theory is developed which will extend standard cosmology by adding a new physical process, which explains the intrinsic-redshifts observed in some galaxies and QSOs.

2.   Redshift quantisation in associated QSOs

Redshifts of QSOs have generally been attributed to the doppler-effect in an expanding universe, and when these objects are uncritically bunched together as a whole there appears to be little sign of periodicity; see Hawkins et al (2002), Tang & Zhang (2005), Duari, Das Gupta & Narlikar (1992), Karlsson (1990). However, certain bright QSOs seen close to nearby active galaxies definitely appear to exhibit redshifts at particular values, see Burbidge (1968, 1973, 1996, 2001), Karlsson (1971, 1977, 1990), Barnothy & Barnothy (1976), Burbidge & Hewitt (1990), Arp et al (1990, 2005), Burbidge & Napier (2001), Napier (2003), Napier & Burbidge (2003), Galianni, et al (2004), Lopez-Corredoira & Gutierrez (2004).

Sometimes the high density of QSOs around some galaxies or the visual alignment or pairing of objects either side of a galaxy is remarkable and is taken as direct evidence for QSO ejection from their parent galaxy; see E.M. Burbidge et al (1971, 2004, 2008), Arp (1971, 1980, 1981, 1983, 1987, 1997a, 1997b, 1998, 1999), Burbidge et al (1990, 2006), Arp et al. (2005, 2008), E.M. Burbidge (1995, 1997), Arp & Fulton (2008). If this be true, then these associated QSOs are probably less massive than the cosmological QSOs seen in galaxy centres which show mainly doppler plus a little gravitational redshift. Associated QSOs sometimes show increasing brightness with redshift, exactly opposite to what one expects for cosmological QSOs, see Arp (1984). This means there must be *two populations of QSOs* which differ in their redshift mechanisms, but are otherwise similar. In their publications, Arp, Burbidge and Karlsson have given several scientific reasons to

support their findings of intrinsic-redshift. The compelling features which need to be investigated in more detail are the causes of intrinsic-redshift and its quantisation, QSO association with galaxies, and alignment of QSO triplets.

Measured redshifts for *associated* QSOs will be taken as being mainly intrinsic, but with some doppler component close to that of the parent galaxy. In addition, relativistic gravitational-redshift is assumed to be small enough to ignore relative to the intrinsic-redshift. Associated QSOs appear to have broad emission-lines similar to cosmological QSOs, so they probably have similar BLR disc structures; see Wayte (2004).

Our theoretical explanation for intrinsic-redshift in stable orbiting bodies is that the gravitational field of the parent galaxy core induces gravito-cordic field formation, as described in Paper 1. This then draws out a catena of electromagnetic energy from atoms, to propagate around the orbit. Consequently, the atoms themselves are left deficient in energy, and effectively redshifted whenever excited to emission; see an extreme example in Arp, Burbidge, & Burbidge, (2004).

For the case of a QSO orbiting within a galactic centre, a subsequent violent ejection will shake-off this extended catenal energy as radiation and leave the deficient QSO outside of the galaxy, where we will observe it as permanently redshifted. No later evolution to a lower redshift state occurs, which would tend to smear the Karlsson periodicity. On average, the observed higher redshifts pertain to those QSOs which were more tightly bound to their parent core, and are now outside but nearer to their parent galaxy.

In work on galaxies, only small values of quantised-redshift have been seen. However, when intrinsic-redshift is large in associated QSOs, it is necessary to quantise in terms of $\ln(1 + z_i)$ rather than z_i itself. This means that the original orbiting catenal energy was a substantial amount of self-energy of the QSO material; so now the reduced mass m_i of a particle without its catenal energy is the source of redshifted photons we observe. Therefore, relative to its original total mass m_o, this is denoted by:

$$\left(\frac{m_i}{m_o} \right) = \left(\frac{1}{1 + z_i} \right) \ , \tag{1}$$

where as usual, $(z_i = (\lambda - \lambda_o)/\lambda_o)$ and $(\lambda/\lambda_o = \nu_o/\nu = m_o/m_i)$. Consequently, after differentiation we shall propose:

$$-\left(\frac{dm_i}{m_i}\right) = d\left[\ln(1+z_i)\right] = \text{constant} \times dN \quad . \tag{2a}$$

Here, dN increases as a fraction of the *current* reduced atomic mass m_i rather than of the *initial* total mass m_o. Integration then gives:

$$\ln(1+z_i) = N \times k_i(\text{constant}) + k_o(\text{constant}) \quad , \tag{2b}$$

where N takes integral values to produce the observed quantisation in $\ln(1 + z_i)$. Observations of associated bright QSOs produce this result in which the proportional constant k_i is the best-fit period at about 0.205, (or 0.089 for $\log_{10}$), see Karlsson (1977), Arp et al (1990). The additional offset constant k_o is typically around 0.06, but it might include cosmological and random doppler redshift for each QSO.

So many observations show this 0.205 period that it must have an atomic foundation, such as:

$$0.205 \approx 1/\ln(137.036), \tag{3}$$

where $(137.036 = \alpha^{-1})$ is the inverse fine structure constant. We can now interpret Eqs.(1) and (2b) by developing an *action* expression for the catenal energy $(m_{cat}c^2)$ emanating from a particle in an associated QSO:

$$\ln\left(\frac{m_o c^2 \tau}{m_i c^2 \tau}\right) = \ln\left(1 + \frac{m_{cat} c^2 \tau}{m_i c^2 \tau}\right) = \ln(1+z_i) \approx \quad .$$

$$\frac{N}{\ln 137} + k_o = N \times \frac{(GMm_o/R)(2\pi R/c)}{\int\limits_{R_o}^{137R_o}(GMm_o/R')(2\pi dR'/c)} + k_o \, . \tag{4}$$

Here the denominator represents the standard *action* necessary to grow a characteristic catena loop from a given QSO particle m_o, under the induction of a parent galaxy core mass M, from radius $(R_o = GM/c^2)$ to $(137 \times R_o)$. This is used to normalise action of the real particle catena loop around the QSO's orbit, over period $(\tau = 2\pi R/c)$. See Landau and Lifshitz (1983) for theory of action integrals, and Wayte (2010b) for analogous theory of electron creation.

Observations give the preferred redshifts of associated QSOs as:

$$z_i \approx 0.06, 0.30, 0.60, 0.96, 1.41, 1.96, 2.63, 3.45 \text{ and } 4.47 \,, \tag{5}$$

see Figure1. The first term is believed to be different in origin from the rest and acts as an offset value, derived in Section 3. The *interval* period is quite precise:

$$\ln(1 + z_{n+1}) - \ln(1 + z_n) \approx 0.205 \ , \tag{6}$$

and although our proposed period Eq.(3) is fairly accurate, greater accuracy would suggest:

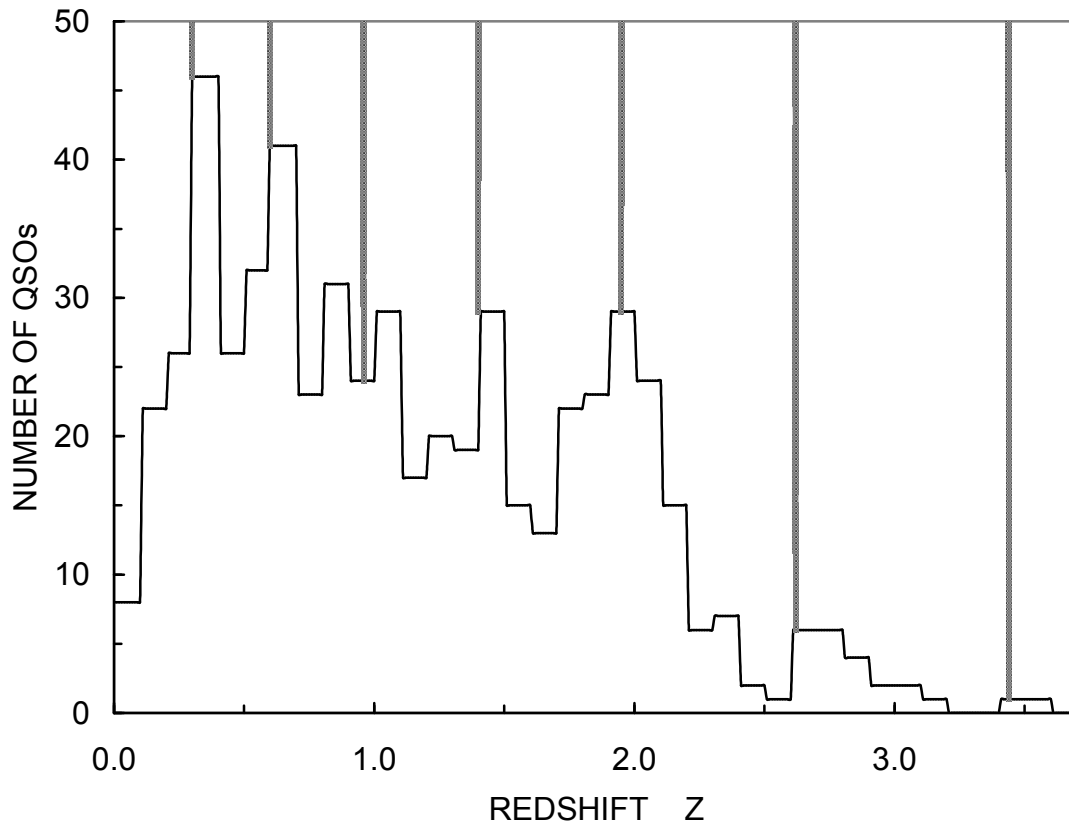$$[-(1 - \alpha) \ln \alpha]^{-1} = 0.20474 \quad . \tag{7}$$

Fig 1   The distribution of 574 QSO emission line redshifts, with added markers at the proposed quantised values. (Data replotted from Karlsson, 1977).

For this, the angle 2π in the denominator of Eq.(4) would have to be reduced to an effective integration angle of $2\pi(137-1)/137$, to match R increasing by $(137-1)R_o$. Consequently, by using Eq.(7) plus Eq.(4), with the second value in Eq.(14b) to set:

$$k_o = \ln(1 + z_o) = 0.0585 \ , \tag{8}$$

then the more accurate observed sequence evaluates as:

$$z_i = 0.060; \ 0.301; \ 0.597; \ 0.959; \ 1.405; \ 1.95; \ 2.62; \ 3.44, \ 4.45. \tag{9}$$

Our final inference will therefore be that z_o should account for the currently-observed QSO's catenal energy around its own BLR disc, whereas z_n in Eq.(6) applies only to the catenal energy of the original pre-ejection QSO around its parent galaxy core.

Parameter N has up till now been independent, so we need to investigate how N is selected as an integer for individual QSOs. Wills et al (1993, figure 9) have plotted the FWHM equivalent velocities for a large number of QSO and quasar emission-line profiles. The mean value corresponds to a HWHM velocity around c/137, presumably because the emitting BLR disc material has a mean velocity near this value. Therefore, in common with the Bohr atom, these very high velocities are possible around dense central masses, and we can derive a reasonable explanation for quantisation in Eq.(4) by direct comparison. Thus, quantisation occurs in the Bohr atom only when the electron orbits contain an integral number of de Broglie wavelengths. Likewise here, let the gravitational de Broglie wavelength for an electron [$\lambda_{GB} = (h/mv)(e^2/Gm^2)^{1/2}$] and Compton wavelength [$\lambda_{GC} = (h/mc)(e^2/Gm^2)^{1/2}$] be fitted into the original QSO orbits around their parent galaxies, in integral quantities only; (here e/m is the electronic charge/mass ratio). A particular condition which has been discovered for average mass spiral galaxies is that the theoretical gravitational circumference is equal to the gravitational de Broglie wavelength of hydrogen; see Paper 1, Eq.(7.3). We shall propose that to get the quantisation here for QSOs, the gravitational circumference of the parent galaxy core mass (M) should be related to the above gravitational Compton wavelength of electrons:

$$2\pi\left(\frac{GM}{c^2}\right) \approx S\lambda_{GC} \text{ ; for integral S.} \tag{10}$$

Then for a straightforward interpretation in the weak *field case*, Eq.(4) may be written:

$$\ln\left(\frac{m_i + m_{cat}}{m_i}\right) \approx \left(\frac{m_{cat}c^2\tau}{m_ic^2\tau}\right) \approx \frac{N \times S \times \left[h \times \left(e^2/Gm^2\right)^{1/2}\right]}{\int\limits_{R_o}^{137R_o}(GMm/R')(2\pi dR'/c)} + k_o \quad . \tag{11}$$

Clearly, the numerator contains a very special quantum of action, and multiplier N may vary if there are several QSOs orbiting around the same parent galaxy core mass. It will be presumed that the more tightly bound QSOs usually have the larger N values, and these will be ejected less distance from the galaxy, on average.

The only obvious interpretation for N is that it represents the number of *coherent* laps that a QSO's catena has around the *galaxy* core, which increase its strength in steps. In Section 6b, this appears to be the explanation for galaxies which orbit in clusters, where N is observed to extend up to 90 times. It will also explain why there are so many examples of paired QSOs with very similar redshifts across parent galaxies, which are the result of ejecting coherent QSO binaries.

As an example, let the mean orbit velocity of a QSO around its parent galaxy be ($v_1 \sim c/137$), then ($\lambda_{GB1}/\lambda_{GC} \sim 137$), and in the simplest example let ($2\pi R_1/\lambda_{GB1} \sim 137$) for an electron mass m_o . This makes the mean effective radius of the orbit equal to ($R_1 \sim 1.48 \times 10^{10}$km), which is 137 times the size of Venus' orbit. At the same time, the parent galaxy core mass is $5.3 \times 10^5 M_\Theta$, and its gravitational radius (GM_1/c^2) is exactly one gravitational Compton radius in Eq.(10). Of course, its actual radius would be greater. [For comparison, our Galaxy has a central core of mass $3.6 \times 10^6 M_\Theta$, see Genzel et al. 2003]. On the left side of Eq.(11), the catenal energy ($m_{cat}c^2$) relative to the reduced mass energy ($m_i c^2$) for the constituent QSO particles is around 20% in this example, (N = S = 1).

Although we have just implied that these QSOs are governed by the electron's gravitational Compton wavelength, we could also use the gravitational de Broglie wavelength in Eq.(10) for much greater M values. Alternatively, the proton-pearls and mesons could also be involved; see Wayte (2010c). Then to keep M in the same range, λ_{GC} would be replaced by their gravitational de Broglie wavelengths. Indeed, a later optical catalogue of 3594 QSOs by Hewitt & Burbidge (1987) reveals a quantisation period of $(\ln 37.7)^{-1}$ operating in some QSOs, rather than $(\ln 137)^{-1}$. This dimensionless constant ($37.7 = 12\pi$) occurs in work on particle physics and is related to 137, (Wayte, 2010b,c). Thus in place of Eq.(4) we get:

$$\ln(1 + z_i) = \frac{N}{\ln 37.7} + k_o \quad . \tag{12}$$

The data is rather selected because of techniques employed in the observations, but nevertheless, Figure 2 shows how peaks do occur at integral values of N, to satisfy Eq.(12) or Eq.(4), when the same offset z_o is included. Calculated values from Eq.(12) are:

$$z_i \approx 0.06, 0.40, 0.84, 1.43, 2.20, 3.21. \tag{13}$$

According to E.M. Burbidge (1995), NGC 4258 has ejected a pair of quasars, with $z_1 = 0.653$ and $z_2 = 0.398$. The first corresponds to N = 2 plus a little doppler shift in Eq.(9), and the second to N = 1 in Eq.(13). Clearly, this application of two laws will make

data-fitting more successful, but raises the question of how one or other is chosen for the original orbit around the parent galaxy core. A random best-fit to the system dimensions could initiate the move to a coherent fit.
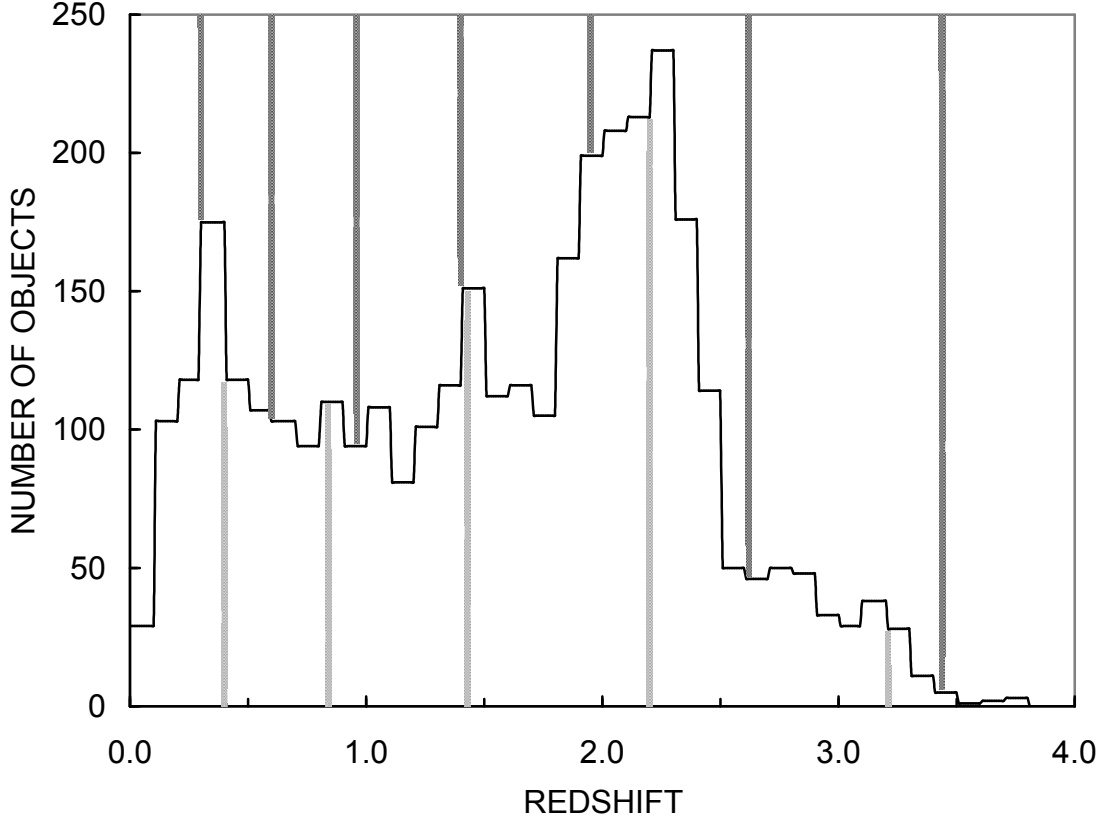

Fig 2   The emission redshift distribution for all 3594 QSOs, with added markers at proposed integral N values, for Eq.(5) (at top) and Eq.(13) (at bottom). (Data replotted from Hewitt & Burbidge, 1987).

3.   The redshift peak at z = 0.06

It was found in Eq.(9) that the offset redshift (z_o ~ 0.0602) was essential in calculating the observed sequence of intrinsic-redshift for all associated QSOs. Consequently, this offset affects all the QSOs to some extent, and must be the result of a different mechanism from that described in the main part of Eq.(4).

Burbidge and Hewitt (1990) investigated the peak at (z ~ 0.06) in the redshift distribution of active galactic nuclei which are *similar* to QSOs in their optical properties. Their data also revealed a strong peak at (z ~ 0.03), plus evidence of weak peaks at (z ~ 0.09, 0.12, 0.18), see Figure 3. We therefore need to interpret their result and then assume that the z ~ 0.06 peak is the one which applies particularly to associated QSOs, but not

necessarily uniquely. The formula which yields a redshift sequence is a variation of Eq.(4), namely:

$$\ln\left(\frac{m_o}{m_i}\right) = \ln(1 + z_i) \approx \frac{N}{\ln 137}\left(\frac{m_\pi}{m_p}\right) = N \times \frac{(GM_{AGN}m_\pi / R)(2\pi R / c)}{137R_o \int\limits_{R_o}(GM_{AGN}m_p / R')(2\pi dR' / c)} \ , \ (14a)$$
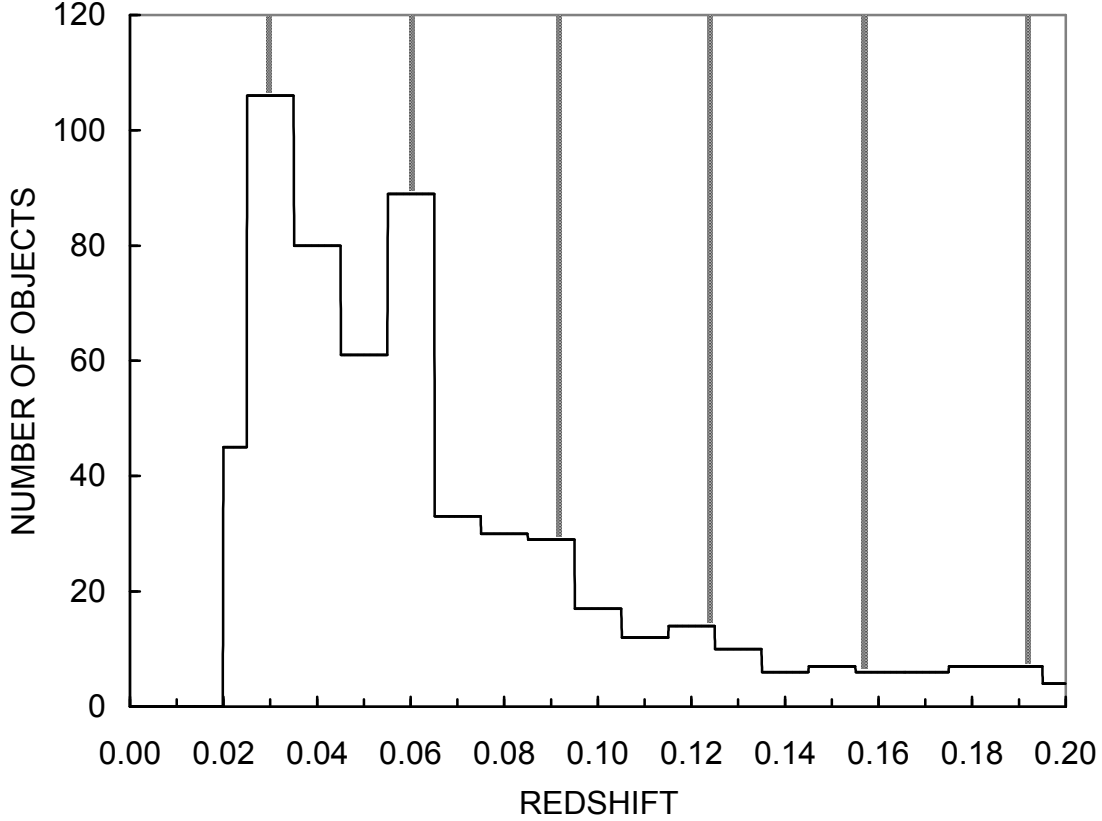

Fig 3   Histogram of the distribution of z for QSO-type objects with 0.02 < z < 0.2; with added markers from Eq.(14b) at integral values of N. (Data replotted from Burbidge & Hewitt, 1990).

Here, the last numerator represents action of catenal energy around the BLR disc, derived from the pionic nuclear field of the protons constituting the *disc material*; see Wayte (2010c). This implies that the proton total mass energy is involved, not just the electronic orbits which determine emission frequencies. The denominator represents the amount of action expended to create a characteristic electromagnetic catena due to central core mass M_{AGN}, rather than the parent galaxy core which it is still orbiting but at a much larger radius. This formula gives, for $(m_p / m_\pi = 6.952)$ and (N = 1, to 6):

$$z_i \approx 0.0297; \; 0.0602; \; 0.0917; \; 0.124; \; 0.157; \; 0.192 \; . \qquad (14b)$$

Arp et al. (1990) have discovered the interesting effect that groups of associated QSOs in different parts of the sky are *systematically offset* in redshift by 0.03 or 0.06. This implies that some of the catena energy spreads from the BLR disc to reach other QSOs in the vicinity, where it encourages formation of similar intrinsic-redshifts. In Section 6, variations of Eq.(14a) will be applied successfully to companion galaxies, and clusters and field galaxies. We shall see that a particular redshift period may be resonant throughout a large region of galaxies, to the exclusion of other periods. This would explain also the QSOs in a given neighbourhood exhibiting a *common offset* value.

4.   QSO absorption lines

Absorption lines in 55 bright QSOs have been accurately observed by Sargent, Boksenberg and Steidel (1988), who concluded that the absorption occurred in galaxies randomly spaced between us and the QSOs. However, Arp et al. (1990) have identified some periodicity in these CIV absorption redshifts, after allowing for varying degrees of offset dependent on the QSO position coordinates.

These objects need to be observed further at different wavelengths because the small spectral range ($\Delta z \sim 0.6$, for CIV) is affecting the statistical analysis, and many strong lines cannot be identified at present. Nevertheless, Figure 4 shows a plot of all the given species of absorption lines, except that obvious clumps of lines within 1000kms^{-1} of each other have been counted as single objects. Apparently, the absorption redshifts are concentrated near the emission line redshifts, and a dearth band then follows beneath. This may mean that the absorbing clouds could be concentrated around the associated galaxies from which they were ejected like QSOs. Four of these QSOs were also observed in the ultraviolet region by Jannuzi et al. (1998) and showed additional absorption lines, mostly due to HI; see open circles in Figure 4. Consequently, there are probably clouds of lower redshift, which could still be associated with the QSOs but are not excited enough to show CIV or other species.
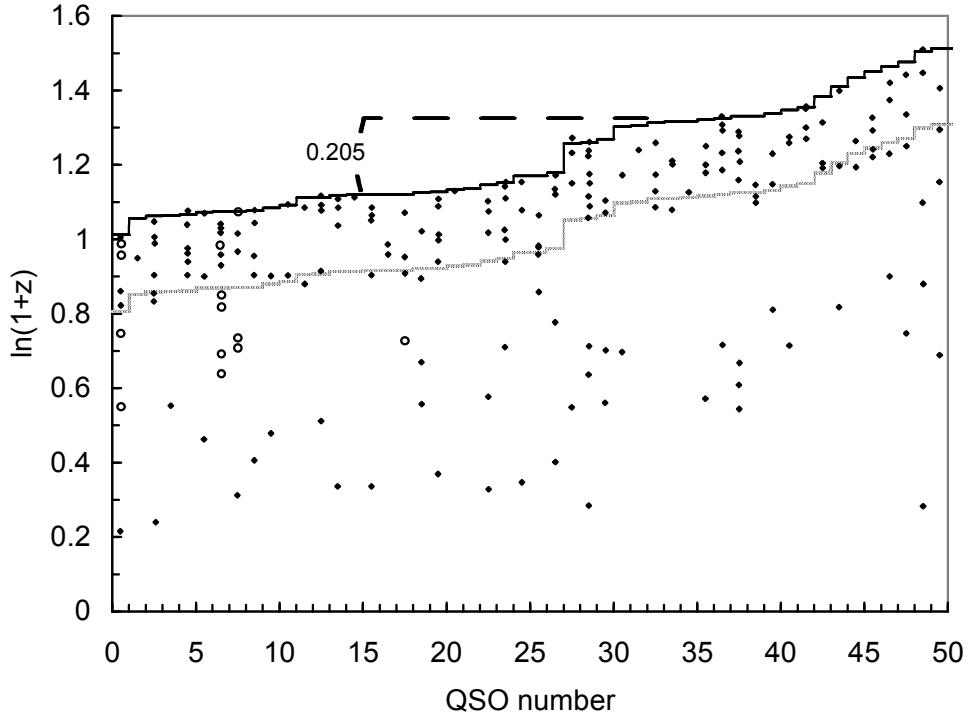
Fig.4 A plot of all species absorption lines in 50 QSOs listed by Sargent, Boksenberg and Steidel (1988), with obvious clumps shown as a single point. The continuous black line follows the *emission line* redshifts, increasing in 50 steps from z = 1.751 to 3.540. The marked step of $\Delta\ln(1+z) = 0.205$ shows how many of the QSOs tend to concentrate around the z = 1.96 and 2.63 values of Eq.(9), when offset of $z_o = 0.03$ from Eq.(14b) has also been included. The theoretical grey line runs at 0.205 below the black line and appears to enclose about two thirds of the total absorption lines. Four of these QSOs were also observed by Jannuzi et al. (1998), as shown by the open circles, mostly due to HI.

5.   QSO association with galaxies

Burbidge et al (1990) have shown how 278 QSO-galaxy pairs prefer certain linear separations, in addition to a general decrease in number density with separation, see histogram in Figure 5 here. A preferred QSO-galaxy separation is apparent at about 90kpc, for their choice of $H_0 = 50 \text{kms}^{-1}\text{Mpc}^{-1}$. By summing their histogram from zero to 200kpc separation, a curve fit may be obtained which approximates to the law:

$$N = 368\left\{1 - \exp\left(-\frac{r}{142}\right)\right\} = N_o\left\{1 - \exp\left(-\frac{r}{R}\right)\right\} \quad , \qquad (15)$$

where $N_o = 368$ is the maximum number of QSOs, and R = 142kpc is the characteristic separation. By differentiating this, a smooth exponential decrease in number density is obtained, as plotted on Figure 5 for ($\Delta r = 20$kpc):

$$\Delta N = \frac{N_o}{R} \exp\left(-\frac{r}{R}\right) \times \Delta r \quad . \tag{16}$$
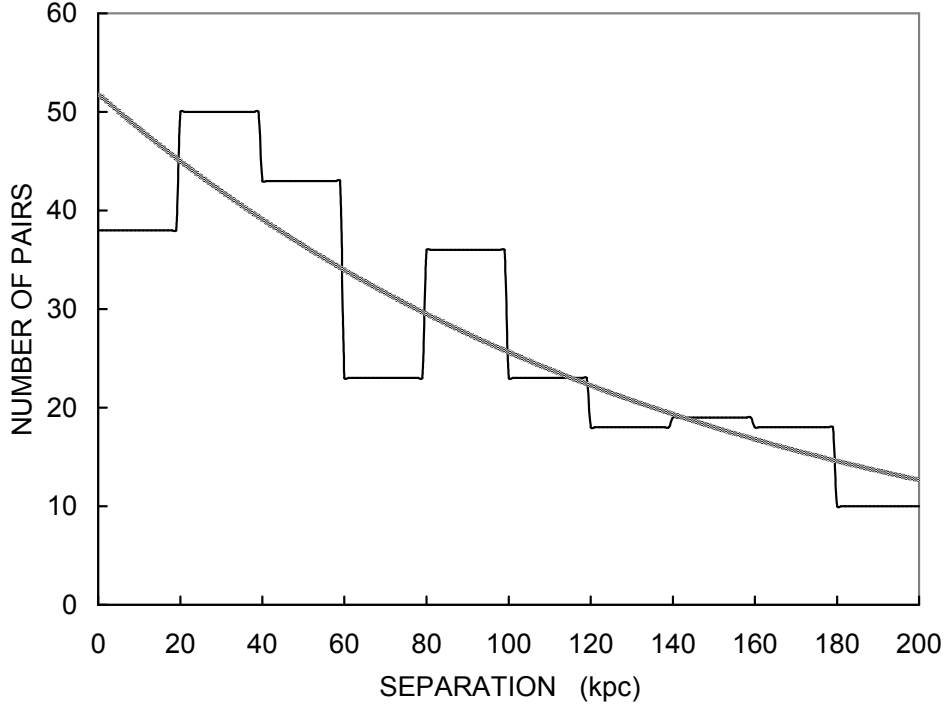

Fig 5   Histogram of the empirical distribution of separations of 278 QSO-galaxy pairs, with added theoretical exponential law. (Data replotted from Burbidge et al. 1990)

The general distribution given by Eq.(15) is equivalent to a spherically symmetric array of 368 QSOs around a single galaxy. Calculation then reveals that such a spherical QSO array would have a volume density ρ_v decreasing with radius as:

$$\rho_v \approx \left(\left(\frac{3}{4}\right)\frac{N_o}{R}\right)\frac{\exp\left(-r/R\sqrt{2}\right)}{4\pi r^2} \quad . \tag{17}$$

Consequently, the corresponding number of QSOs in a spherical shell of thickness Δr is:

$$\Delta n \approx \left(\left(\frac{3}{4}\right)\frac{N_o}{R}\right)\exp\left(\frac{-r}{R\sqrt{2}}\right) \times \Delta r \quad . \tag{18}$$

This has the appearance of a diffusion law distribution for QSOs ejected from parent galaxies, which cannot be attributed to random statistical pairing. If the QSO redshifts

were actually cosmological rather than intrinsic, then distant QSOs would appear to be concentrated behind galaxies which are near to us.

6. Intrinsic-redshift in galaxies

In Section 3 it was shown how a QSO orbiting a parent galaxy is encouraged by the gravito-cordic field to emit its catena of electromagnetic energy around its orbit. This leaves the QSO body and BLR disc deficient in energy, and therefore only able to emit the redshifted photons we observe. By analogy, companion galaxies orbiting around massive central galaxies or groups of galaxies are induced to emit their catena and become relatively redshifted. This intrinsic-redshift has been observed for many years by Tifft, Arp and others, and will now be interpreted in 3 categories as follows.

6a. *Intrinsic-redshift period around 72kms^{-1}*

A substantial body of evidence has been accumulated for this intrinsic-redshift period; see a review by Tifft (1995) and references therein, Arp and Sulentic (1985) with references. More recently, Napier (2003) has evaluated high-precision data on 48 spirals in the Virgo cluster, and discovered a period of 71kms^{-1} for differential redshifts, by power spectrum analysis. This is probably the same effect as discovered by Tifft in the Coma cluster and Arp in companion galaxies, at 72kms^{-1}, although further observations would be necessary to be sure. We can derive a theoretical model for action of this intrinsic-redshift directly from Eq.(4), in the form:

$$\ln(1+z_i) \approx \frac{N}{(2\pi 137) \times \ln 137} = \frac{N}{137} \times \frac{(GM_g m_o / 2\pi R)(2\pi R / c)}{\int_{R_o}^{137R_o} (GM_g m_o / R')(2\pi dR' / c)} \quad . \tag{19}$$

This produces a period of 70.77kms^{-1} which could be increased to 71.3kms^{-1} by applying the modification of Eq.(7). Coefficient (1/137) is a scale factor for this particular phenomenon, which involves the self-interaction in orbiting galaxies around the massive Virgo cluster centre. Radius R could represent the effective orbit radius of a galaxy within the cluster. The denominator represents a theoretical characteristic action required for creation by spiralling open the galactic material from radius R_o to 137R_o.

Since factor N is clearly shown up to 25 cycles in Napier's data, an explanation is that the catena extends N times around the orbit and builds its energy in steps for each

coherent orbit (2πR). This could be easier for the spiral galaxies with a strong internal gravito-cordic field, see Paper 1. Then the phase of the orbiting gravito-cordic field and catena settles into a single value for all N orbits. Such a model is strongly supported by the fact that irregular galaxies show no intrinsic-redshift periodicity.

Although Eq.(19) describes the intrinsic-redshift in any single galaxy, all the 48 spirals in the Virgo cluster appear to agree with this, allowing for some random velocity doppler-shift. This implies that the gravito-cordic field is resonant throughout the cluster, at the fundamental frequency; see Paper 1 for resonance effects in spiral galaxies. Other frequencies then tend to be excluded while the resonance grows, as the galaxies settle into their stable states.

Sub-harmonic resonance of Eq.(19), for N = ½ , ⅓ , corresponding with redshift periods of 36, 24kms^{-1}, are theoretically possible in different groups of galaxies, see Tifft and Cocke (1984).

6b.   *Intrinsic-redshift period around 36kms^{-1} or 37.5km^{-1}*

Again, a great amount of evidence has been obtained for this redshift period; see Tifft (1995), Tifft & Cocke (1984), in particular. The inference from this and other sub-multiples of 72kms^{-1} is that there is a progression of periods (24→36→72kms^{-1}), for galaxies with high 21cm flux levels, as profile width increases. Physically it may mean that in Eq.(19), N = ⅓ is less probable than N = ½ , which is less probable than N = 1, so calmer galactic material is necessary to produce the 24 and 36 kms^{-1} redshift periods.

Napier (2003) has evaluated differential redshifts for high-precision data on 89 galaxies in 28 groups (each containing 2-6 companions) scattered over the sky throughout the Local Supercluster. The power distribution in the 28 groups has a well-defined maximum at 37.5kms^{-1}. This periodicity appears to be global throughout the LSC, rather than just local to the individual groups. However, the periodicity is strongest for the galaxies linked by group membership. No periodicity was found for a sample of 62 irregular galaxies.

This period was detectable out to at least 90 cycles within the LSC, and its accuracy implies that it should not be confused with the 36kms^{-1}, discussed above. A formula to describe this period is quite similar to Eq.(19), namely:

$$\ln(1+z_i) \approx \frac{N/2}{6 \times 137 \times \ln 137} \approx \frac{N/2}{137} \times \frac{(GM_g m_o / 6R)(6R/c)}{\int\limits_{R_o}^{137R_o} (GM_g m_o / R')(6dR'/c)} \quad . \tag{20}$$

This produces a period of 37.055kms^{-1} which could be increased to 37.33kms^{-1} by again applying Eq.(7). To explain this, it is necessary to imagine a field of many galaxies in a roughly hexagonal array. Then let one particular galaxy be chosen to be at the origin of coordinates, and the distance between centres be R. So the perimeter joining the 6 surrounding galaxies is of length 6R. This length has therefore replaced $2\pi R$ previously used for the circular catena in Eq.(19). We shall infer that the gravito-cordic field and catena in field galaxies propagate rectilinearly from galaxy to galaxy, being deflected in a controlled way to preserve phase across the resonating LSC. The additional factor 2 implies that the electromagnetic catena *intensity* rather than amplitude is governing the overall process. Although the actual galaxies are not in physical contact, this hexagonal array must exist roughly, allowing for random velocities. Small groups of galaxies show this phenomenon more strongly but the data shows that even in the LSC overall, global resonance is still managing to operate. It is impossible to tell whether the hexagonal format originated from the Big Bang particle structure, or began in the condensing diffuse material under the influence of an early spontaneous gravito-cordic field, (see Paper 1, Section 7.3).

6c. *Intrinsic-redshift period 1000 - 20,000kms^{-1}*

Several papers have been published on *discordant redshifts* ($\Delta cz > 1000 \text{kms}^{-1}$), for example see Arp (1997c) and references therein. The brightest galaxies in compact groups have the lowest redshift and are presumed to be the most massive, generally. So the fainter less-massive galaxies have greater redshift and probably orbit the central massive galaxy. These excess redshifts are therefore presumed to be intrinsic and due to the catenal energy, as can be described by a variation of Eq.(14a):

$$\ln(1+z_i) \approx \frac{N}{2\pi \ln 37.7}\left(\frac{m_\ell}{m_p}\right) = N \times \frac{(GM_g m_\ell / 2\pi R)(2\pi R/c)}{\int\limits_{R_o}^{37.7R_o} (GM_g m_p / R')(2\pi dR'/c)} \quad , \tag{21}$$

Here, the scale factor 37.7 is believed to derive from some involvement of the proton substructure in generating the catenal energy, with ($m_\ell = m_p/9$) being the proton-pearl mass, see Wayte (2010c). Then the last numerator represents self-interaction of catenal

energy around the galaxy orbit, derived from the constituent pearls of the protons which constitute the galaxy. The denominator represents the amount of action expended to create a characteristic electromagnetic catena due to galaxy mass M_g. This formula gives intrinsic redshifts, which fit Arp's data fairly well for (N = 1, 2, 3, 4, 5, 7, 12):

$$cz_i \approx 1464; \ 2936; \ 4414; \ 5900; \ 7393; \ 10401; \ 18050 \ kms^{-1}. \qquad (22)$$

7.   K-Trumpler effect

This anomalous redshift effect has been observed for over 95 years, and has recently been reviewed by Arp (1992). The belief, common to all these experienced astronomers, has been that it represents real intrinsic-redshift in stars, since doppler and gravitational redshift explanations do not work. Overall, the conclusion is that the most luminous stars, in spectral class from O – M, have the largest redshifts. If these are the most massive stars, then the effect increases with gravitational field in the outer layers that we observe. This means that the interior gravito-cordic field is strong, as will be the catenal energy circulating within the star and also propagating externally around the cluster to which it belongs. Rotation of the stars is probably a crucial feature in the emission of catenas, as it was for the rotating and orbiting galaxies discussed above. The suggestion by Narlikar and Arp (1993) that the intrinsic-redshift is due to younger age of the luminous star material raises the question as to how these stars formed from a cloud of younger material in the same vicinity as the older material in dwarf stars.

Actual values of intrinsic-redshift vary too much to say whether the above process in Eq.(19) is involved with sub-harmonics due to fractions in place of integral N. Usually, the excess redshift is less than 20kms^{-1}, but occasionally values are higher. If scale-factor (m_π / m_p) or (m_ℓ / m_p) could be put in Eq.(19), then N could remain an integer and cover the observations. Calculated values will need to allow for any outflow velocity due to mass-loss adding some blue-shift. Turbulence velocities will also tend to smear any periodicity.

8. Conclusion

Emission of a gravito-cordic field and electromagnetic catena from orbiting bodies represent additional phenomena in gravitational theory, rather than a modification of it. They are generated and propagate azimuthally around orbits, under the control of normal gravity acting radially.

Intrinsic-redshift in associated QSOs has been attributed to an energy-defect in their atoms, due to their catenal energy being unavailable for spectral processes. Their large amount of intrinsic-redshift was quantised by an "action principle" which operated around their original parental orbit. The constant of proportionality which links different QSOs is determined by the fine structure constant (1/137) or a related function (1/37.7), according to an action principle. The linear separations of many QSO-galaxy pairs have been analysed to reveal a distribution with the appearance of a diffusion law, as if the QSOs really were ejected from their associated parent galaxies.

An intrinsic-redshift period at 71kms^{-1}, observed in galaxies in the Virgo cluster, has been interpreted as being proportional to their orbital catenal energy around the massive cluster centre. For galaxies in the Local Supercluster, the intrinsic-redshift period at 37.5kms^{-1} implies the existence of catenal energy resonating throughout an array of galaxies.

The K-Trumpler effect in stars has been interpreted as intrinsic-redshift, which increases with mass and luminosity due to stronger catenal energy.

Acknowledgement

References

Arp, H. 1971, Science 174, 1189-1200

Arp, H. 1980, ApJ, 236, 63-69

Arp, H. 1981, ApJ, 250, 31-42

Arp, H. 1983, ApJ, 271, 479-506

Arp, H. 1984, ApJ, 285, 555-566

Arp, H. 1987, Quasars, Redshifts, and Controversies. (Berkeley: Interstellar Media)

Arp, H. 1992, MNRAS, 258, 800-810

Arp, H. 1997a, A&A, 328, L17-L20

Arp, H. 1997b, J. Astrophys. Ast. 18, 393-406

Arp, H. 1997c, ApJ, 474, 74-83

Arp, H. 1998, ApJ, 496, 661-9

Arp, H. 1999, ApJ, 525, 594-602

Arp, H. and Sulentic, J. W. 1985, ApJ, 291, 88-111

Arp, H., et al. 1990, A&A, 239, 33-49

Arp, H., Burbidge, EM., Burbidge, G., 2004, arxiv:astro-ph/0401007

Arp, H., et al. 2005, arxiv:astro-ph 0501090

Arp, H. and Fulton, C. 2008, arxiv:astro-ph: 0803.2591v1

Barnothy, J. M. and Barnothy, M.F. 1976, PASP, 88, 837-841

Burbidge, E. M. 1995, A&A, 298, L1-L4

Burbidge, E. M. 1997, ApJ, 484, L99-L101

Burbidge, E. M., et al. 1971, ApJ, 170, 233-244

Burbidge, E. M., et al. 2004, ApJS, 153, 159-163

Burbidge, E. M. et al. 2005, arxiv:astro-ph: 0510815

Burbidge, G. R. 1968, ApJ. Lett., 154, L41-L48

Burbidge, G. R. 1973, Nature, 246, 17- 19

Burbidge, G. R. 1996, A&A, 309, 9-22

Burbidge, G. R. 2001, Pub. Astr. Soc. Pac., 113, 899-902

Burbidge, G. and Hewitt, A. 1990, ApJ, 359, L33-L36

Burbidge, G. and Napier, W.M. 2001, ApJ, 121, 21-30

Burbidge, G. et al. 1990, ApJS, 74, 675-730

Burbidge, G. et al. 2006, arxiv:astro-ph/0605140v1

Duari, D., Das Gupta, P., and Narlikar, J. V. 1992, ApJ, 384, 35-42

Freedman, W. L., et al. 2001, ApJ, 553, 47-72

Galianni, P. et al. 2004, arxiv:astro-ph/0409215

Genzel, R. et al. 2003, Nature, 425, 934-937

Hawkins, E., Maddox, S. J., Merrifield, M. R. 2002, MNRAS, 336, L13

Hewitt, A., and Burbidge, G. 1987, ApJS, 63, 1-246

Karlsson, K. G. 1971, A&A, 13, 333-335

Karlsson, K. G. 1977, A&A, 58, 237-244

Karlsson, K. G. 1990, A&A, 239, 50-56

Landau, L. D. and Lifshitz, E. M. 1983, The classical theory of fields, 4th ed,
        Pergamon Press, Oxford, section 16

Lopez-Corredoira, M. & Gutierrez, CM., 2004, arxiv:astro-ph/0401147

Napier, W.M. 2003, ApSS, 285, 419-427

Napier, W. M. and Burbidge, G. R. 2003, MNRAS, 342, 601

Narlikar, J. and Arp, H. 1993, ApJ, 405, 51-56

Ratcliffe, H. 2009, www.vixra.org/abs/0907.003

Sargent, W. L. W., Boksenberg, A. and Steidel, C. C. 1988, ApJS, 68, 539-641

Tang, S. M. and Zhang, S. N. 2005, ApJ, 633, 41-51

Tifft, W. G. 1995, ApSS, 227, 25-39

Tifft, W. G., and Cocke, W. J. 1984, ApJ, 287, 492-502

Wayte, R. 2004, Astronomical & Astrophysical Trans, 23, 1-33

Wayte, R. 2010a (Paper 1) www.vixra.org/abs/1002.0018

Wayte, R. 2010b www.vixra.org/abs/1007.0055

Wayte, R. 2010c www.vixra.org/abs/1008.0049

Wills B J, et al 1993 ApJ. 415, 563-579